European Radiology (2019) 29:1074–1082
https://doi.org/10.1007/s00330-018-5629-2

GASTROINTESTINAL

Radiomics nomogram for predicting the malignant potential of gastrointestinal stromal tumours preoperatively

Tao Chen[1,2] · Zhenyuan Ning[3] · Lili Xu[4] · Xingyu Feng[5] · Shuai Han[6] · Holger R. Roth[2] · Wei Xiong[4] · Xixi Zhao[4] · Yanfeng Hu[1] · Hao Liu[1] · Jiang Yu[1] · Yu Zhang[3] · Yong Li[5] · Yikai Xu[4] · Kensaku Mori[2] · Guoxin Li[1]

Received: 23 May 2018 / Revised: 16 June 2018 / Accepted: 22 June 2018 / Published online: 16 August 2018

Abstract

Objective To develop and evaluate a radiomics nomogram for differentiating the malignant risk of gastrointestinal stromal tumours (GISTs).

Methods A total of 222 patients (primary cohort: n = 130, our centre; external validation cohort: n = 92, two other centres) with pathologically diagnosed GISTs were enrolled. A Relief algorithm was used to select the feature subset with the best distinguishing characteristics and to establish a radiomics model with a support vector machine (SVM) classifier for malignant risk differentiation. Determinant clinical characteristics and subjective CT features were assessed to separately construct a corresponding model. The models showing statistical significance in a multivariable logistic regression analysis were used to develop a nomogram. The diagnostic performance of these models was evaluated using ROC curves. Further calibration of the nomogram was evaluated by calibration curves.

Results The generated radiomics model had an AUC value of 0.867 (95% CI 0.803–0.932) in the primary cohort and 0.847 (95% CI 0.765–0.930) in the external cohort. In the entire cohort, the AUCs for the radiomics model, subjective CT findings model, clinical index model and radiomics nomogram were 0.858 (95% CI 0.807–0.908), 0.774 (95% CI 0.713–0.835), 0.759 (95% CI 0.697–0.821) and 0.867 (95% CI 0.818–0.915), respectively. The nomogram showed good calibration.

Conclusions This radiomics nomogram predicted the malignant potential of GISTs with excellent accuracy and may be used as an effective tool to guide preoperative clinical decision-making.

Key Points

- *CT-based radiomics model can differentiate low- and high-malignant-potential GISTs with satisfactory accuracy compared with subjective CT findings and clinical indexes.*
- *Radiomics nomogram integrated with the radiomics signature, subjective CT findings and clinical indexes can achieve individualised risk prediction with improved diagnostic performance.*
- *This study might provide significant and valuable background information for further studies such as response evaluation of neoadjuvant imatinib and recurrence risk prediction.*

Tao Chen and Zhenyuan Ning contributed equally to this work.

Electronic supplementary material The online version of this article (https://doi.org/10.1007/s00330-018-5629-2) contains supplementary material, which is available to authorized users.

✉ Tao Chen
drchentao@163.com

✉ Guoxin Li
gzliguoxin@163.com

[1] Department of General Surgery, Nanfang Hospital, Southern Medical University, Guangdong Provincial Engineering Technology Research Center of Minimally Invasive Surgery, No.1838, North Guangzhou Avenue, Guangzhou 510515, Guangdong Province, China

[2] Graduate School of Information Science, Nagoya University, Furo-cho, Chikusa-ku, Nagoya 464-8603, Japan

[3] School of Biomedical Engineering, Southern Medical University, Guangzhou 510515, Guangdong Province, China

[4] Medical Image Center, Nanfang Hospital, Southern Medical University, Guangzhou 510515, Guangdong Province, China

[5] Department of General Surgery, Guangdong General Hospital, Guangdong Academy of Medical Science, Guangzhou 510080, Guangdong Province, China

[6] Department of General Surgery, Zhujiang Hospital, Southern Medical University, Guangzhou 510280, Guangdong Province, China

Keywords Gastrointestinal stromal tumour · Classification · Radiomics · Nomogram · Machine learning

Abbreviations

AFIP	Armed forces institute of pathology
AUC	Area under curve
CI	Confidence interval
EVFDM	Enlarged vessels feeding or draining the mass
GISTs	Gastrointestinal stromal tumours
ICCs	Inter- and intraclass correlation coefficients
NCCN	National comprehensive cancer network
NIH	National institutes of health
OR	Odds ratio
SVM	Support vector machine

Introduction

Gastrointestinal stromal tumours (GISTs) are the most common mesenchymal tumours in the gastrointestinal tract [1, 2]. GISTs are clinically heterogeneous, exhibiting varying degrees of malignant potential in individual patients [3]. Furthermore, evaluating the biological behaviour of GISTs preoperatively is important for surgical decision-making [4]. However, the difficulty of assessing a tumour's malignant potential and the increasing incidence of GISTs present challenges to surgeons.

The National Institutes of Health (NIH) modified criteria [5], the Armed Forces Institute of Pathology (AFIP) criteria [6] and others have been proposed for use in risk prediction. However, these criteria are applied postoperatively because the mitosis count of the specimen is a significant factor in these criteria. Clinical symptoms, tumour size and computed tomography (CT) findings are helpful and often used together in the preoperative risk stratification of GISTs [7–9], providing synthetic evidence for decision support. Nevertheless, these subjective assessments are likely affected by an individual observer and may perform insufficiently when faced with tumour heterogeneity.

On the other hand, machine learning (ML) has become a hot topic with reports of breakthroughs not only in industry and finance but also medical care support. Radiomics, as a typical case of medical application of machine learning, has attracted increasing attention in recent years [10]. Previous studies indicated that radiomics features can be used to assess the biological behaviour of a tumour comprehensively, which may potentially improve the accuracy of diagnosis, prognosis and prediction [10–13].

To our knowledge, whether the radiomics approach is superior for predicting the malignant potential of GISTs has not been evaluated. Moreover, to integrate the radiomics signature, clinical factors and the conventional CT examinations in order to fully assess and effectively support the preoperative clinical management, we aim to establish and validate a radiomics-based prediction nomogram for the patients with GISTs in this study.

Patients and methods

Patients

Approved by the institutional review board, this retrospective study enrolled 222 patients with histologically confirmed GISTs from three centres, and patient informed consent was waived. From January 2007 to December 2015, a total of 130 patients (72 men and 58 women; mean age, 57 ± 12.48 years) from our centre were identified and comprised the primary cohort. The inclusion criteria were as follows: (1) patients who underwent surgery for GISTs with curative intent; (2) patients underwent standard contrast-enhanced CT less than 15 days before surgical resection; (3) patients with complete clinicopathologic data. The exclusion criteria were as follows: (1) patients received imatinib therapy or other tyrosine kinase inhibitor as a neoadjuvant before surgery; (2) tumour ruptured during the operation. The patient recruitment pathway is presented in Fig. S1. All patients underwent standard contrast-enhanced CT scans before surgery. An external validation cohort of 92 patients (67 patients from Guangdong General Hospital, and 25 patients from Zhujiang Hospital; 41 men and 51 women; mean age, 60 ± 11.44 years) was acquired using the same criteria from January 2011 to December 2015.

Demographic and clinicopathologic data, including age, gender, tumour site, size of the tumour (maximum diameter) and mitotic count, were derived from medical records. The NIH modified criteria were used to stratify the malignant potential of GISTs on the basis of the clinical and postoperative histological index, as a verification of our model (low malignant potential, very low risk and low risk; high malignant potential, intermediate risk and high risk) [5].

CT image acquisition, three-dimensional segmentation of tumour images and radiomics feature extraction

CT image acquisition and retrieval procedure are described in Supplementary S1. Three-dimensional (3D)

segmentation of the region of interest (ROI) was performed using ITK-SNAP 3.6 (ITK-SNAP 3.X TEAM) (Fig. 1). Feature extraction method was applied to the ROI in MATLAB 2016b (Mathworks) with feature extraction algorithms implemented. Because the CT images were from different centres with different scan parameters, preprocessing of the ROI images, including wavelet bandpass filtering, isotropic resampling and quantisation of grey level are applied before the texture feature extraction process (Supplementary S2).

Interobserver reliability and intraobserver reproducibility of feature extraction were analysed with the whole data in a blind fashion by two radiologists with 12 (reader 1, W.X.) and 7 years (reader 2, X.X.Z.) of experience in the interpretation of abdominal CT. An independent samples *t* test was used to evaluate the differences between the features generated by reader 1 and those by reader 2 (interobserver), as well as between the twice-generated features by reader 1 (intraobserver). Inter- and intraclass correlation coefficients (ICCs) were used to evaluate the agreement of features extraction. There is a good agreement when the ICC is greater than 0.75. All technicians were blinded to clinical data. Aiming to normalise the data of different magnitudes, eliminate the negative effects of large differences of magnitudes and make the subsequent analysis more reliable, we applied the min–max scaling method to all features extracted.

Feature selection and radiomics model building

The feature subset with the best distinguishing characteristics for the radiomics model was obtained using the Relief algorithm [14] and exhaustive test based on the performance of the support vector machine (SVM) classifier [15] (Supplementary S3). First, the unordered features were ranked from the most important to the least important. Then, different feature sets could be obtained using the exhaustive test from the ordered sequence $1 \leq m \leq M$. The set of first m features was fed into the SVM classifier, and its performance for differentiating low- and high-malignant-potential GISTs was evaluated on the basis of receiver operating characteristic (ROC) curves and the area under the curve (AUC). A subset with the highest AUC was selected as the optimal feature subset for the discrimination task.

Statistical analyses

Clinicopathologic data

Statistical analyses of clinicopathologic data are described in Supplementary S4.

Clinical index and subjective CT findings model

Univariate analysis was applied to compare the differences of the clinical indexes between the two groups by using a chi-square test or the Fisher's exact test, where appropriate. A binary logistic regression analysis was subsequently applied to build the clinical index model using the significant variables from the univariate analysis as inputs. Odds ratios (OR) as estimates of relative risk with 95 % confidence intervals (CI) were obtained for each risk factor. The statistical analysis of the subjective CT findings model was the same as with the clinical index model. The analysis was performed in SPSS (SPSS statistic 22, IBM).

Radiomics analysis and nomogram development

ROC curve and other indices including AUC, threshold, specificity and sensitivity were calculated using the "Hmisc" package in R software (version 3.4.2, R Core Team). The reducing method Relief and classifier SVM were performed in MATLAB 2016b (Mathworks) supplemented with the machine learning package. ICCs were also calculated in MATLAB with the "ICC.m" function. Nomogram and calibration curve were analysed using the "rms" package in R.

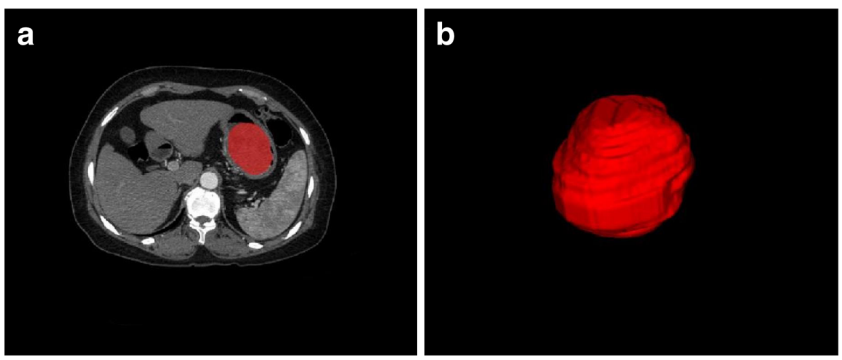

Fig. 1 Three-dimensional segmentation of GISTs. **a** Manual segmentation on the axial slice. **b** Three-dimensional volumetric reconstruction

Clinical index analyses

The candidate indicators for clinical index model include age, gender, tumour site (gastric or non-gastric), maximum tumour diameter (≤ 5 cm or > 5 cm) and clinical symptoms. Gastrointestinal haemorrhage, abdominal mass, ileus, and abdominal pain, which are the major symptoms in GIST patients, were recorded in this study [2]. The maximum tumour diameter was acquired before surgery on the basis of clinical assessment.

Subjective CT findings evaluation

The subjective CT findings for each case were independently assessed and recorded in a blinded manner by two experienced radiologists (W.X. and X.X.Z.; readers 1 and 2, with 12 and 7 years of experience in the interpretation of abdominal CT, respectively). In the event of disagreement, the two readers jointly reviewed the findings to reach a consensus for further analysis.

The CT imaging characteristics included in this study were sorted as follows: tumour shape (irregular or regular); tumour margin (poorly or well-defined); density (hypodensity or isodensity); calcification (present or absent); growth patterns (uniform or mixed); severe necrosis (present or absent); enhancement type (homogenous or heterogeneous); level of enhancement (mild/moderate or marked); enlarged vessels feeding or draining the mass (EVFDM, present or absent); direct organ invasion (present or absent); and lymphadenectasis (present or absent) [7]. The uniform growth pattern was defined as endoluminal or exophytic. Severe necrosis was considered greater than 50% tumour necrosis. These features were assessed as previously described [7, 16].

Development of a radiomics nomogram and comparison of different models

The significant predictors of clinical index, subjective CT findings and radiomics signature were entered into the logistic regression analysis to build the combined model using a nomogram, which was provided for the clinician as a quantitative tool [17]. The calibration of the radiomics-based nomogram was assessed using calibration curves [13, 18].

The diagnostic performance of the radiomics model, the subjective CT findings model, the clinical index model and the radiomics nomogram for differentiating low- and high-malignant-potential GISTs was evaluated on the basis of ROC curves and AUC values. Differences in the AUC values between the four models were assessed using the Delong test.

Results

Clinical characteristics

There were no significant differences in the distribution of low- and high-malignant-potential cases in the two cohorts (p = 0.785). The characteristics of the patients in the primary and external cohorts are provided in Table 1 and Supplementary S5.

Feature extraction, selection and radiomics model building

In total, 10,320 features were extracted from the tumour ROI with satisfactory inter- and intraobserver reproducibility assessments (Table S3 and Supplementary S6). The prediction performances obtained by each model composed of different initial feature subsets are presented in Fig. 2a. The optimal feature subset consisted of 10 features (Table 2) that achieved excellent performance in GIST risk stratification, yielding AUC values of 0.867 (95% CI 0.803–0.932) and 0.847 (95% CI 0.765–0.930) in the primary cohort and external cohort, respectively (Fig. 2b and Supplementary S7).

Clinical index analyses

Regarding age, gender, tumour site and abdominal pain, no differences were observed between the low- and high-malignant-potential groups (p > 0.05). However, for maximum tumour diameter and clinical symptoms, including gastrointestinal haemorrhage, ileus and abdominal mass, statistical significance was found between these two groups (p = 0.000, 0.002, 0.001 and 0.002, respectively). Significant clinical features in the univariate analysis were included in the binary logistic regression to build a clinical index model, and the results of the logistic regression revealed significant differences only in the maximum tumour diameter and gastrointestinal haemorrhage (both p < 0.05).

Subjective CT findings model building

In the univariate analysis, tumour shape, tumour margin, severe necrosis, growth pattern, enhancement type, EVFDM, direct organ invasion and lymphadenectasis were significantly different between the low- and high-malignant-potential GISTs (p < 0.05), but no significant differences were found in other subjective features between the two groups, including density, calcification and the level of enhancement (p = 0.863, 0.466 and 0.378, respectively). The binary logistic regression analysis showed that only growth pattern and EVFDM remained as independent risk factors for malignant

Table 1 Patient characteristics in the primary and external cohorts

Characteristics	Primary cohort		*p*	External cohort		*p*
	Low-malignant-potential GISTs	High-malignant-potential GISTs		Low-malignant-potential GISTs	High-malignant-potential GISTs	
Age, mean ± SD, years	54.52 ± 11.73	59.52 ± 12.81	0.022*	60.02 ± 11.89	59.68 ± 11.12	0.887
Gender, no. (%)			0.583			0.389
Male	35 (53.0)	37 (57.8)		18 (40.0)	23 (48.9)	
Female	31 (47.0)	27 (42.2)		27 (60.0)	24 (51.1)	
Primary site			0.480			0.672
Stomach	51 (77.3)	46 (71.9)		37 (82.2)	37 (78.7)	
Non-stomach	15 (22.7)	18 (28.1)		8 (17.8)	10 (21.3)	
Tumour size, cm	3.27 ± 1.17	8.16 ± 4.72	< 0.001*	2.90 ± 1.54	8.43 ± 5.06	< 0.001*
Mitotic count			< 0.001*			< 0.001*
≤ 5/50 HPF	66 (100.0)	31 (48.4)		45 (100.0)	21 (44.7)	
> 5/50 HPF	0 (0.0)	33 (51.6)		0 (0.0)	26 (55.3)	

p value is derived from the univariable association analyses between each characteristic and potential malignancy. Independent samples *t* test was applied in continuous variables. Chi-squared test was applied in categorical variables

GISTs gastrointestinal stromal tumours, *SD* standard deviation, *HPF* high-power field

* *p* value < 0.05

potential (both $p < 0.001$). Tumours with EVFDM (odds ratio [OR], 6.737; 95% CI 2.681–16.930) or a mixed growth pattern (OR, 4.672; 95% CI 2.255–9.680) were likely to be higher-risk GISTs than those without the presence of EVFDM or with a uniform growth pattern.

Radiomics nomogram building and performance of different models

The radiomics signature, tumour diameter, gastrointestinal haemorrhage, growth pattern and EVFDM were incorporated

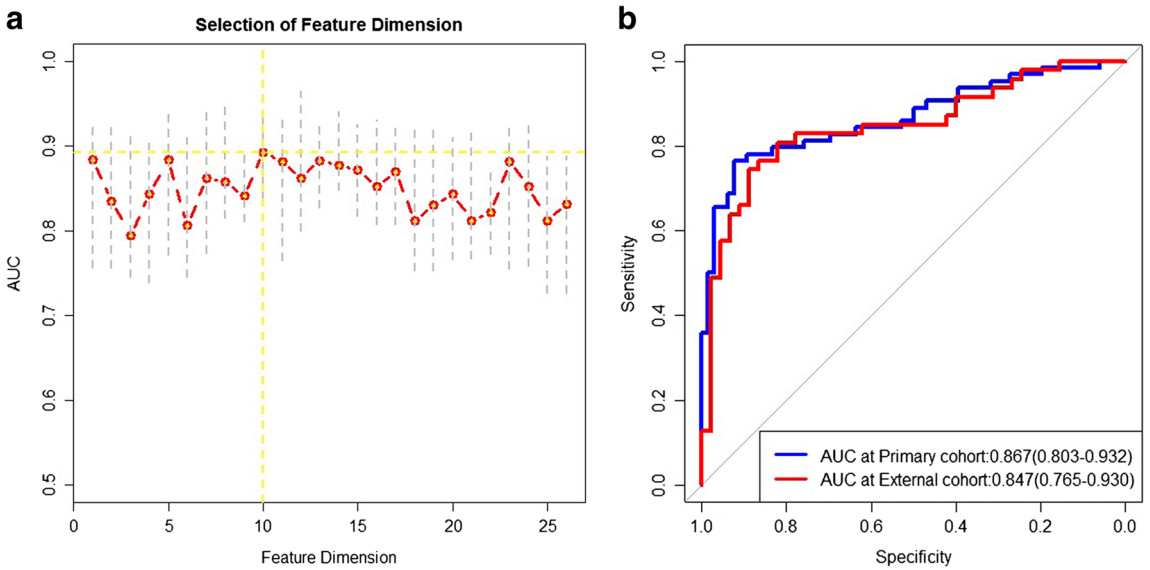

Fig. 2 Selection of feature subsets and the receiver operating characteristic (ROC) curves of optimal feature subset. **a** Classification of performance using different subsets of ranking features: the y-axis represents the value of the area under the ROC curve (AUC); the x-axis represents the dimension of different initial feature subsets; the optimal feature subset ranked consisted of 10 features and achieved the max AUC. **b** ROC curves of the optimal feature subset for the primary and external cohorts

Table 2 Optimal feature subset of radiomics model

Feature	Wavelet bandpass filtering	Isotropic voxel size	Quantisation algorithm	Quantised grey level
NGTDM/strength	0.5	5 mm	Equal	64
GLSZM/GLV	0.5	4 mm	Equal	64
NGTDM/coarseness	1.5	5 mm	Lloyd	64
GLRLM/GLV	1.5	4 mm	Equal	64
GLSZM/GLV	2	5 mm	Equal	64
NGTDM/strength	2	5 mm	Equal	64
NGTDM/strength	1	5 mm	Equal	64
NGTDM/coarseness	1	5 mm	Lloyd	64
GLSZM/GLV	2	4 mm	Equal	64
NGTDM/strength	1.5	5 mm	Equal	64

NGTDM neighbourhood grey-tone difference matrix, *GLV* grey-level variance, *GLSZM* grey-level size zone matrix, *GLRLM* grey-level run-length matrix

into the radiomics nomogram building (Fig. 3). Figure 4 shows that the radiomics nomogram has a good calibration. The diagnostic performance for each model is shown in Fig. 5. The radiomics nomogram achieved a higher AUC (0.867 [95% CI 0.818–0.915]) than the radiomics model (AUC, 0.858 [95% CI 0.807–0.908]), the subjective CT findings model (AUC, 0.774 [95% CI 0.713–0.835]) and the clinical index model (AUC, 0.759 [95% CI 0.697–0.821]). The AUC of the radiomics model was higher than that of the subjective CT findings model and the clinical index model (p = 0.002 and 0.012, respectively); however, no significant difference in AUC values was found between the subjective CT findings model and the clinical index model (p = 0.676). The accuracy of nomogram, radiomics, subjective CT findings and clinical index models are 0.830, 0.811, 0.752 and 0.712, respectively.

Discussion

In this study, we developed an individualised radiomics nomogram for malignancy differentiation for GISTs, which achieved satisfactory discrimination and has the potential to act as a reproducible imaging marker for the decision-making support in a noninvasive and effective way.

Tumour size is a significant factor for evaluating the biological behaviour of GISTs. The National Comprehensive

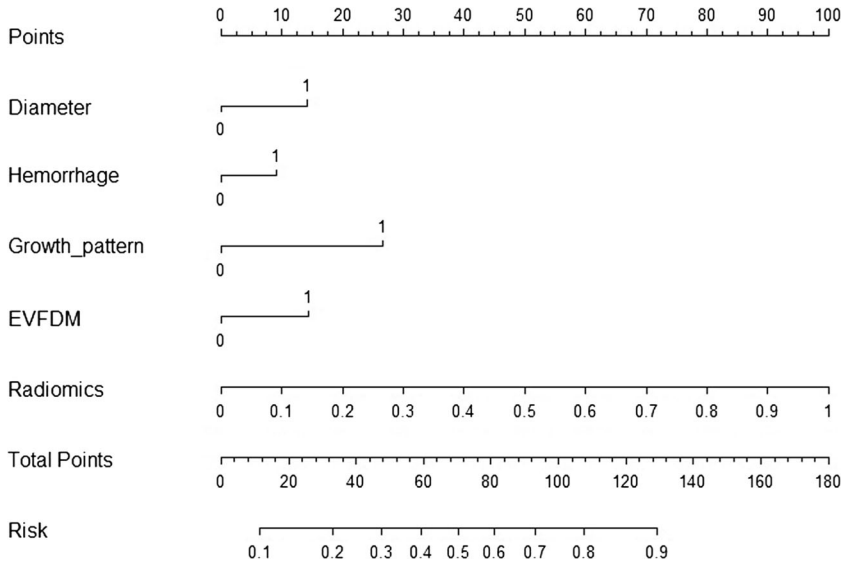

Fig. 3 Developed radiomics nomogram. The radiomics signature, tumour diameter, gastrointestinal haemorrhage, growth pattern and EVFDM were used for building the radiomics nomogram. The probability of each predictor can be converted into scores according to the first scale "Points" at the top of the nomogram. After adding up the scores of these predictors in "Total Points", the corresponding prediction probability at the bottom of the nomogram is the malignancy of the tumour. The cutoff point of our nomogram is 0.69. The case would be diagnosed as high malignant potential when the total prediction probability is beyond the cutoff point

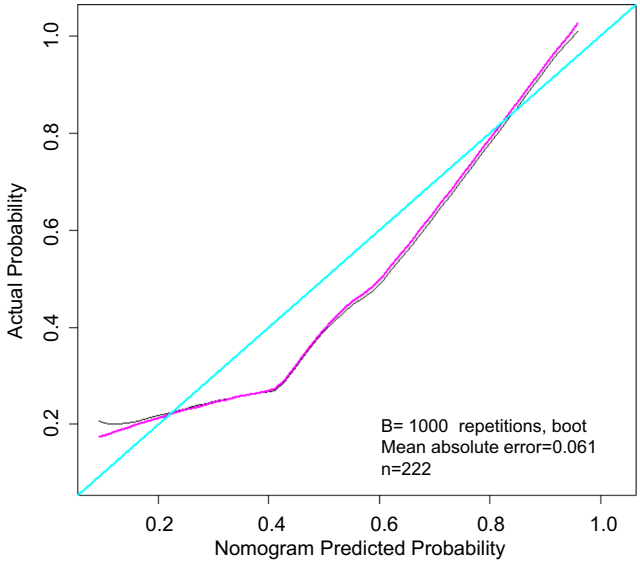

Fig. 4 Calibration curve for the radiomics nomogram. The calibration of the radiomics nomogram was depicted by the calibration curve in terms of the agreement between the predicted risks of GISTs and the actual results based on the modified criteria. The turquoise line represents an ideal prediction, and the purple line represents the predictive performance of the nomogram. The closer the fit of the purple line to the ideal line, the better the prediction. The black line represents the bias corrected

Cancer Network (NCCN) guideline recommends that GISTs larger than 2 cm should undergo surgical resection, whereas tumours with smaller size can be excised or monitored by endoscopy [19]. Nevertheless, evaluating the malignancy of GISTs only by tumour size is insufficient because some small GISTs may be aggressive and have a poor prognosis [20, 21].

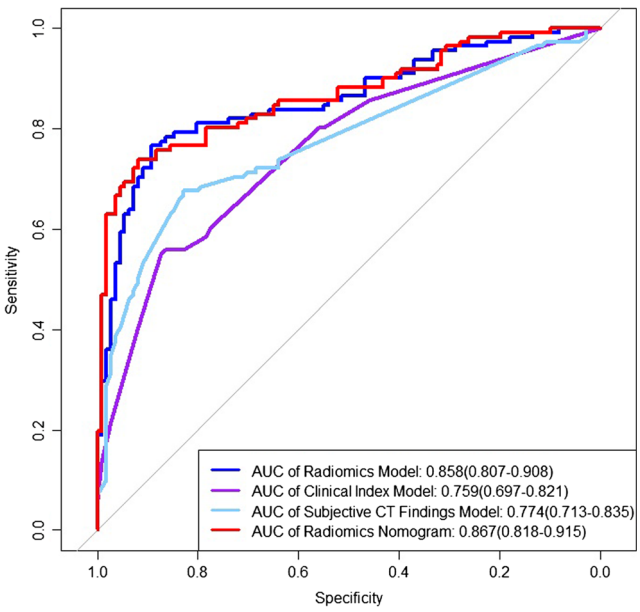

Fig. 5 Receiver operating characteristic (ROC) curves of different models. The four colours of the curves represent different models: dark blue, radiomics model; light blue, subjective CT findings model; red, radiomics nomogram; purple, clinical index model

Therefore, a more effective assessment method is required for closing surveillance of these small tumours exhibiting high malignancy. Associated symptoms can help surgeons intuitively predict the risk of GISTs. Haemorrhage is one of the major symptoms in GIST patients [2]. Previous studies have noted that GIST patients with GI bleeding are more likely to experience tumour recurrence, indicating a poor prognosis [9, 22]. In our study, tumour size and haemorrhage were significantly different between the low- and high-malignant-potential groups in logistic regression. However, when these factors were integrated into the clinical index model, they were much less significant than our radiomics model. In our data, two high-malignant-potential cases with a tumour size less than 3 cm were diagnosed accurately by the radiomics model, but they were underestimated by the clinical index model. It demonstrated that our radiomics model might have the potential to perform better preoperatively in some cases with small tumour size. When the size is greater than 3 cm, the total number miscategorised in the clinical index model is still higher than in the radiomics model. Although our radiomics model is based on texture feature, which does not rely on tumour size, it could work as a complement of size for GIST risk assessment.

CT is a widely available imaging modality for the pretreatment assessment of GIST patients. A previous study noted that CT features are predictors of risk stratification for GISTs [7]. However, compared with the subjective CT findings, our radiomics model shows greater predictive power as indicated by a higher AUC value. There were more overestimated and underestimated cases in the CT assessment than in the radiomics analysis. It demonstrated that our radiomics approach based on the quantitative analysis of image features has an advantage over the subjective CT findings.

Further integrating the radiomics model with these subjective clinical and imaging features using a nomogram can achieve improved diagnostic performance with good calibration. The role of the radiomics-based nomogram in our study is to integrate the clinical factors and the conventional radiological examinations together to provide synthetic evidence. What is more, it can present a quantitative analysis for disease diagnosis and stratification that is superior to conventional approaches.

Although the quantitative radiomics has enormous potential to improve cancer treatment by fully exploiting the intratumour information and assisting in a precise and personalised intervention, a few inherent challenges still exist. Standardisation of the medical image is the primary problem for radiomics for the sake of routine clinical application. In our study, the min–max scaling method was applied to normalise the features extracted. Furthermore, compared with most previous radiomics analyses using data from only one centre, external validation was applied in this study with patient data sets from different institutions, yielding more reliable results.

Furthermore, compared with some previous radiomics analyses in which the features were extracted from the cross-sectional area, analyses using volumetric ROI can provide more abundant information about the tumour because all of the available slices are taken into consideration, which may improve the discrimination accuracy [13, 23–25]. Therefore, radiomics based on volumetric ROIs may be extremely suitable for examining GISTs, one of the most typical solid tumour types with intratumour heterogeneity.

However, a limitation of our study is the retrospective data collection and thus further prospective research is needed. Additionally, parameter adjustment was time-consuming in model building. Nevertheless, this radiomics-based nomogram can easily be programmed into accessible software or websites, which would also facilitate its wide clinical application. More importantly, our radiomics nomogram with the excellent SVM classifier achieved satisfactory discrimination performance, which will bring benefits for the preoperative decision-making regarding GISTs. Moreover, these results provide important background information for further studies in this field. For example, with the exception of the surgical timing assessment, this method may provide additional evidence for the risk evaluation of the patients who have already received neoadjuvant imatinib and whose mitotic count may become less reliable in the postoperative pathological examination under the influence of imatinib. In addition, this methodology may have an important role in the response evaluation of neoadjuvant chemotherapy considering the existing limitation of the current RECIST and Choi criteria [26, 27]. As we know, the RECIST criteria mainly rely on the size of lesion, which might be inferior to the radiomics signature according to the results of the comparison between the radiomics and tumour size in this study. Density is the most critical factor in the Choi criteria, but is susceptible to be interfered. Our radiomics approach that can extract abundant and diversified features for quantitative analysis might supplement the insufficiency of the Choi criteria. Furthermore, our prospective research on the radiomics nomogram for predicting recurrence risk after surgery is ongoing. In the future, we will consider genomic characteristics, such as *KIT* and *PDGFRA* mutations [28], to establish a more comprehensive radiogenomics model.

In conclusion, our study presented a radiomics-based nomogram that showed satisfactory performance in distinguishing low- and high-malignant-potential GISTs. As a more objective and noninvasive technique, quantitative radiomics analysis may be an effective tool to supplement the conventional approaches for the preoperative clinical decision-making process.

Funding This study has received funding by the State's Key Project of Research and Development Plan (2017YFC0108300 and 2017YFC0108303) and JSPS KAKENHI Grant (17H00867 and 26108006).

Compliance with ethical standards

Guarantor The scientific guarantor of this publication is Tao Chen.

Conflict of interest The authors of this manuscript declare no relationships with any companies whose products or services may be related to the subject matter of the article.

Statistics and biometry One of the authors has significant statistical expertise: Hao Liu, Department of General Surgery, Nanfang Hospital, Southern Medical University, Guangdong Provincial Engineering Technology Research Center of Minimally Invasive Surgery, Guangzhou 510515, Guangdong Province, China. Hao Liu has completed postdoctoral research of cancer epidemiological statistics in Heidelberg Cancer Center, Germany. Hao Liu specialises in statistical analysis and provided statistical advice in this study.

Informed consent Written informed consent or substitute was obtained from all patients in this study.

Ethical approval Institutional review board approval was obtained.

Methodology
- retrospective
- diagnostic or prognostic study
- multicentre study

References

1. Nishida T, Blay JY, Hirota S, Kitagawa Y, Kang YK (2016) The standard diagnosis, treatment, and follow-up of gastrointestinal stromal tumors based on guidelines. Gastric Cancer 19:3–14
2. Joensuu H, Hohenberger P, Corless CL (2013) Gastrointestinal stromal tumour. Lancet 382:973–983
3. Shah R, Jonnalagadda S (2005) The GIST of a stromal tumor. Gastroenterology 128:2170–21714
4. Nishida T, Kawai N, Yamaguchi S, Nishida Y (2013) Submucosal tumors: comprehensive guide for the diagnosis and therapy of gastrointestinal submucosal tumors. Dig Endosc 25:479–489
5. Joensuu H (2008) Risk stratification of patients diagnosed with gastrointestinal stromal tumor. Hum Pathol 39:1411–1419
6. Miettinen M, Lasota J (2006) Gastrointestinal stromal tumors: pathology and prognosis at different sites. Semin Diagn Pathol 23:70–83
7. Zhou C, Duan X, Zhang X, Hu H, Wang D, Shen J (2016) Predictive features of CT for risk stratifications in patients with primary gastrointestinal stromal tumour. Eur Radiol 26:3086–3093
8. Burkill GJ, Badran M, Al-Muderis O et al (2003) Malignant gastrointestinal stromal tumor: distribution, imaging features, and pattern of metastatic spread. Radiology 226:527–532
9. Liu Q, Li Y, Dong M, Kong F, Dong Q (2017) Gastrointestinal bleeding is an independent risk factor for poor prognosis in GIST patients. Biomed Res Int. https://doi.org/10.1155/2017/7152406
10. Verma V, Simone CB 2nd, Krishnan S, Lin SH, Yang JZ, Hahn SM (2017) The rise of radiomics and implications for oncologic management. J Natl Cancer Inst. https://doi.org/10.1093/jnci/djx055
11. Gillies RJ, Kinahan PE, Hricak H (2016) Radiomics: images are more than pictures, they are data. Radiology 278:563–577
12. Wu S, Zheng J, Li Y et al (2017) A radiomics nomogram for the preoperative prediction of lymph node metastasis in bladder cancer. Clin Cancer Res 23:6904–6911

13. Huang YQ, Liang CH, He L et al (2016) Development and validation of a radiomics nomogram for preoperative prediction of lymph node metastasis in colorectal cancer. J Clin Oncol 34:2157–2164
14. Kononenko I (1994) Estimating attributes: analysis and extensions of RELIEF. In: Bergadano F, De Raedt L (eds) Machine Learning: ECML-94. ECML 1994. Lecture Notes in Computer Science (Lecture Notes in Artificial Intelligence), vol 784. Springer, Berlin, pp 171–182
15. Noble WS (2006) What is a support vector machine? Nat Biotechnol 24:1565–1567
16. Brancatelli G, Federle MP, Grazioli L, Blachar A, Peterson MS, Thaete L (2001) Focal nodular hyperplasia: CT findings with emphasis on multiphasic helical CT in 78 patients. Radiology 219:61–68
17. Iasonos A, Schrag D, Raj GV, Panageas KS (2008) How to build and interpret a nomogram for cancer prognosis. J Clin Oncol 26: 1364–1370
18. Han DS, Suh YS, Kong SH et al (2012) Nomogram predicting long-term survival after d2 gastrectomy for gastric cancer. J Clin Oncol 30:3834–3840
19. von Mehren M, Randall RL, Benjamin RS et al (2016) Soft tissue sarcoma, Version 2.2016, NCCN Clinical Practice Guidelines in Oncology. J Natl Compr Cancer Netw 14:758–786
20. Nishida T, Goto O, Raut CP, Yahagi N (2016) Diagnostic and treatment strategy for small gastrointestinal stromal tumors. Cancer 122: 3110–3118
21. Tanaka J, Oshima T, Hori K et al (2010) Small gastrointestinal stromal tumor of the stomach showing rapid growth and early metastasis to the liver. Dig Endosc 22:354–356
22. Lv A, Li Z, Tian X et al (2013) SKP2 high expression, KIT exon 11 deletions, and gastrointestinal bleeding as predictors of poor prognosis in primary gastrointestinal stromal tumors. PLoS One. https://doi.org/10.1371/journal.pone.0062951
23. Ng F, Kozarski R, Ganeshan B, Goh V (2013) Assessment of tumor heterogeneity by CT texture analysis: can the largest cross-sectional area be used as an alternative to whole tumor analysis? Eur J Radiol 82:342–348
24. Kickingereder P, Gotz M, Muschelli J et al (2016) Large-scale radiomic profiling of recurrent glioblastoma identifies an imaging predictor for stratifying anti-angiogenic treatment response. Clin Cancer Res 22:5765–5771
25. Chapiro J, Duran R, Lin M et al (2015) Identifying staging markers for hepatocellular carcinoma before transarterial chemoembolization: comparison of three-dimensional quantitative versus non-three-dimensional imaging markers. Radiology 275:438–447
26. Benjamin RS, Choi H, Macapinlac HA et al (2007) We should desist using RECIST, at least in GIST. J Clin Oncol 25:1760–1764
27. Dudeck O, Zeile M, Reichardt P, Pink D (2011) Comparison of RECIST and Choi criteria for computed tomographic response evaluation in patients with advanced gastrointestinal stromal tumor treated with sunitinib. Ann Oncol 22:1828–1833
28. Joensuu H, Wardelmann E, Sihto H et al (2017) Effect of KIT and PDGFRA mutations on survival in patients with gastrointestinal stromal tumors treated with adjuvant imatinib an exploratory analysis of a randomized clinical trial. JAMA Oncol 3:602–609